

## H I SYNTHESIS OBSERVATIONS OF THE ELLIPTICAL GALAXY NGC 4278

ERNST RAIMOND

Netherlands Foundation for Radio Astronomy

S. M. FABER<sup>1</sup>

Lick Observatory, Board of Studies in Astronomy and Astrophysics, University of California, Santa Cruz

J. S. GALLAGHER III

Department of Astronomy, University of Illinois

AND

G. R. KNAPP

Owens Valley Radio Observatory, California Institute of Technology

Received 1980 August 11; accepted 1980 December 15

### ABSTRACT

The hydrogen-rich elliptical galaxy NGC 4278 has been mapped in 21 cm line radiation with the Westerbork Synthesis Radio Telescope. The hydrogen is distributed in an irregular ring within the optical galaxy with a minimum diameter of 15 kpc. The velocity field of the gas is rather regular and indicates ordered rotation about the central galaxy. However, the kinematic major and minor axes deviate from perpendicularity by 15°, indicating that noncircular motions are present. The new data confirm previous conclusions that the rotation of the outer gaseous ring is not coplanar with the rotation of the inner optical galaxy.

The apparent skewing of the kinematic major and minor axes is most easily accounted for by assuming that the gas moves in oval orbits in a barred potential field. However, because the outer gas does not rotate like the inner galaxy, the origin of such a bar is uncertain. Alternatively, we may be seeing a transient, nonequilibrium configuration resulting from the recent capture of a gas cloud or a dwarf irregular galaxy. A warp model and a model based on a tidal perturbation are also considered but look less attractive at the present time.

*Subject headings:* galaxies: individual — galaxies: internal motions — galaxies: structure — radio sources: 21 cm radiation

### I. INTRODUCTION

Unlike most spirals, elliptical galaxies as a class contain no detectable neutral hydrogen. A number of exceptions have been observed (for a list, see Gouguenheim 1979). Of these, NGC 4278 is one of the most prominent examples.

Until now, hardly any information was available concerning the spatial distribution of the hydrogen in these exceptional galaxies. There are at least four reasons why detailed H I observations of gas-rich ellipticals might be scientifically rewarding:

i) Although the statistics are very scanty, there are indications that a correlation exists between nuclear activity and hydrogen “richness” among ellipticals (Gallagher *et al.* 1977; Knapp, Gallagher, and Faber 1978; Fosbury *et al.* 1978; Gunn 1979). H I observations might therefore provide a clue to the origin of nuclear activity.

ii) If we can follow the neutral hydrogen to sufficiently large distances from the center, we have an

independent way of determining the mass of the galaxy and hence the integrated mass-to-light ratio. This is a quantity not easily measured for most ellipticals.

iii) Earlier observations (Knapp, Kerr, and Williams 1978) have shown that the hydrogen gas in the outer regions of NGC 4278 does not rotate like the stars in the inner, optical galaxy. Better observations might shed light on this puzzling phenomenon.

iv) Finally, there is the important question of the origin of the gas. Is it of a primordial nature and therefore part of the galaxy since its inception, or has it been acquired by the galaxy relatively recently?

The present synthesis observations of NGC 4278 were obtained in hopes of addressing these questions.

### II. OBSERVATIONS

#### a) Synthesis Observations

The elliptical galaxy NGC 4278 was observed with the Westerbork Synthesis Radio Telescope combined with a digital spectrometer. The telescope has been

<sup>1</sup>Alfred P. Sloan Foundation Fellow.

described by Baars and Hooghoudt (1974) and Casse and Muller (1974) and the general method of data processing by Högbom and Brouw (1974), while Bos, Raimond, and Van Someren Gréve (1981) describe the digital spectrometer, its performance, and the specific methods of handling the data.

The parameters used for the observations are listed in Table 1. Because of the low surface brightness expected in the line, angular resolution was sacrificed in favor of better sensitivity per synthesized beam by using only half the WSRT array. After correcting the data for baseline misalignment, etc., the complex gain of every frequency channel on each interferometer was determined by means of calibration observations of 3C 147 and 3C 309.1 made just before and after each of the two 12 hr syntheses of NGC 4278.

Maps with a spatial resolution of  $49 \times 103$  arc seconds ( $\alpha \times \delta$ ) were made independently at 31 radial velocities spaced by  $32.98 \text{ km s}^{-1}$ . Each of these was convolved to a circular beam of  $103''$  half-power diameter. Subsequently a "continuum" map was obtained by averaging the 10 channel maps at velocities  $221\text{--}353 \text{ km s}^{-1}$  and  $947\text{--}1079 \text{ km s}^{-1}$ , which were considered free of 21 cm radiation from either NGC 4278 or our Galaxy and which were also sufficiently far removed from the edges of the instrumental passband. The continuum map is dominated by a point source of approximately 500 mJy at the nucleus of NGC 4278. The hydrogen line maps shown in Figure 1 were produced by subtracting the continuum map from the original maps. A Hanning taper function, applied in the lag-to-frequency transform, caused each of the original maps to be 50% correlated with its neighbor. Therefore, all information is contained in the set of maps shown, although twice as many were available originally.

Summation of the maps in the velocity range  $419\text{--}815 \text{ km s}^{-1}$  resulted in Figure 2*a*, showing the distribution of neutral hydrogen in the galaxy. The same distribution superposed on a Hale telescope prime-focus photograph, kindly put at our disposal by James E. Gunn, is shown in Figure 5*a* (Plate 5). Figure 2*b* was produced by

summation of the original full-resolution maps in all areas where the brightness temperature of the corresponding smoothed maps exceeded  $0.15 \text{ K}$  (approximately two times rms noise). This procedure discriminates against faint unresolved features not confirmed by the smoothed maps.

As we felt that the original elongated beam distorted the appearance of the distribution unacceptably and because of the poor signal-to-noise ratio of the unsmoothed maps, we based most of our analysis on the smoothed distributions. However, the unsmoothed maps were used whenever the best possible angular resolution was required (e.g., in deriving the velocity field).

One of the most prominent features in the total hydrogen distribution is the apparent minimum in the center. Although it is conceivable that absorption of the radiation of the nuclear source could contribute to the central depression in the distribution, it seems unlikely that it can account for all or even most of it. If the hole were caused by absorption alone, it should be exactly centered on the continuum source in all of the individual maps. Also the velocity range over which it could be seen would probably be relatively small. Neither one of these conditions is fulfilled. However, the steep velocity gradient (see Fig. 3) across the central part of the galaxy will cause the signal from any H I present to be spread over many channel maps, thereby reducing its detectability. For example, if the hydrogen was spread evenly over  $360 \text{ km s}^{-1}$ , the column density would have to exceed  $7.7 \times 10^{19} \text{ cm}^{-2}$  in order to be detected on the individual channel maps and to be included in the total H I summation. As this is obviously a very extreme case, the actual central column density lies between the apparent value of approximately  $4.5 \times 10^{19} \text{ cm}^{-2}$  and  $7.7 \times 10^{19} \text{ cm}^{-2}$ . We therefore conclude that there is a real minimum in the neutral hydrogen distribution near the center.

The apparent distribution of the gas is consistent with either a spheroidal or a flattened, disklike geometry. Measurements of the velocity dispersion, presented below, show that the ratio of random to circular velocities

TABLE 1  
SUMMARY OF INSTRUMENTAL PARAMETERS

|   |  |
|---|--|
| Frequency of center of band .....                   | 1417.222 MHz   |
| Radial velocity (with respect to the Sun) .....     | $650 \text{ km s}^{-1}$                                  |
| Overall band width .....                            | 5 MHz ( $1105 \text{ km s}^{-1}$ )                       |
| Field center coordinates ( $\alpha, \delta$ ) ..... | $184^{\circ}35, 29^{\circ}50$ (1950.0)                   |
| Coordinates of NGC 4278 ( $\alpha, \delta$ ) .....  | $184^{\circ}40, 29^{\circ}558$ (1950.0)                  |
| Dates of observation .....                          | 1979 July 7–8  |
| Length of observation .....                         | $2 \times 12 \text{ hr}$                                 |
| Baselines (on E-W line) .....                       | 36, 72, 108, ..., 684, 720 m                             |
| Synthesized beamwidth .....                         | $49.4 \times 103.1 \text{ arc sec}$ ( $\alpha, \delta$ ) |
| Synthesized band width .....                        | $66 \text{ km s}^{-1}$                                   |
| Rms noise in individual unsmoothed channel maps ... | 0.70 mJy per beam or 0.11 K                              |
| Rms noise after smoothing .....                     | 0.34 mJy per beam or 0.05 K                              |

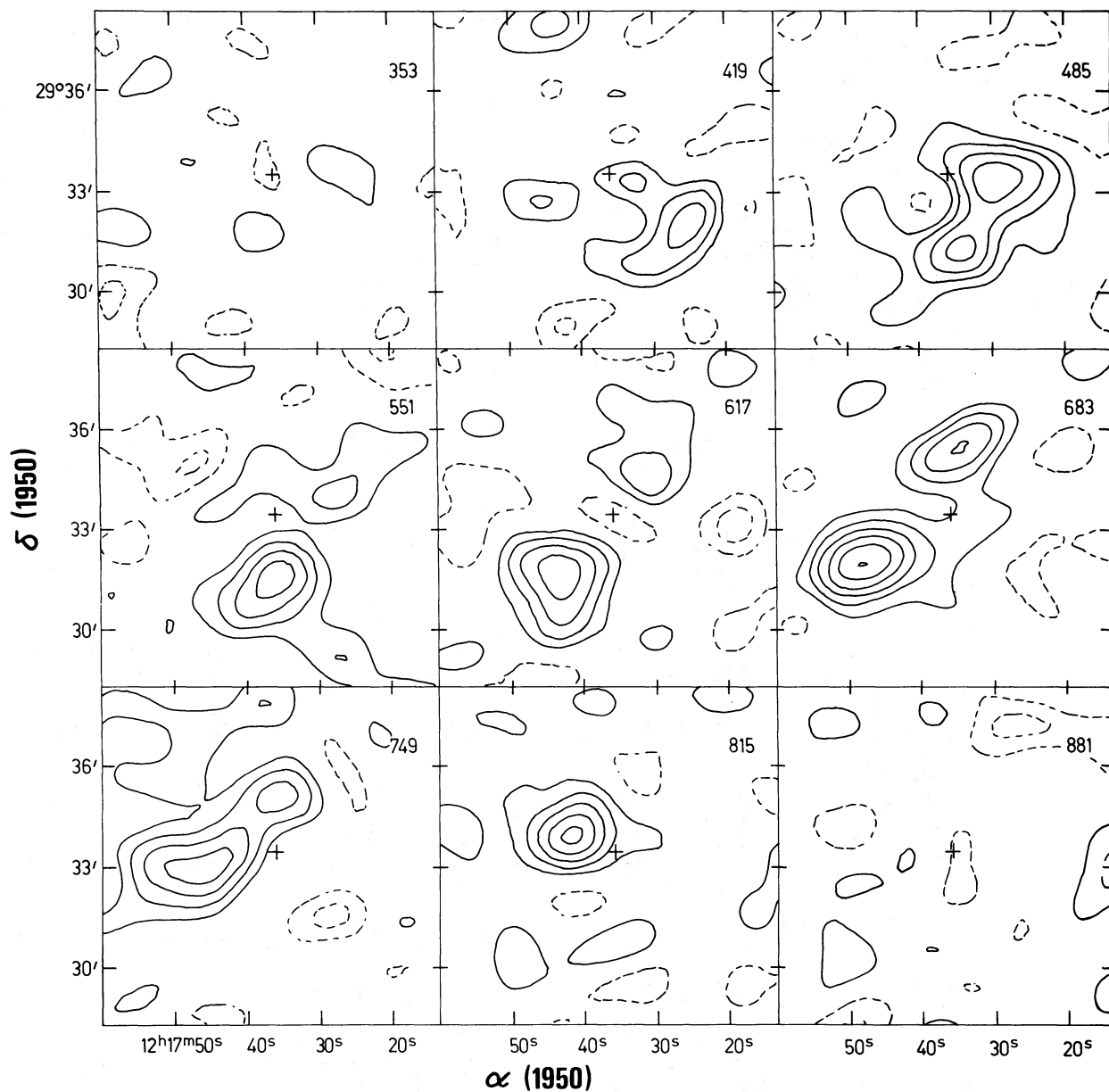


FIG. 1.—Synthesis maps of the 21 cm brightness distribution of NGC 4278. The original maps obtained with a resolution of  $49 \times 103$  arc seconds ( $\alpha \times \delta$ ) have been convolved to a circular beam of  $103''$  half-power diameter. The heliocentric radial velocity is indicated in the upper right-hand corner of each map. The contour interval is 0.1 K, negative contours are indicated by dashed lines, and the zero contour is not shown. The rms noise in the map is approximately 0.05 K. The cross in the center indicates the position of the point source of about 0.5 Jy in the nucleus of NGC 4278.

is less than about 0.2. The gas is therefore probably in a flattened system.

Figure 3 is a cut through the three-dimensional ( $\alpha, \delta, V$ ) cube of full-resolution data along the apparent kinematical major axis of the hydrogen ring. Its position angle is  $65^\circ$ . A more complete picture of the distribution of the radial velocities is given by the velocity field. Two versions are shown in Figures 4a and 4b. The first was

obtained by calculating the mean velocity weighted by the local hydrogen distribution at each point in the map and plotting isovelocity contours. The second one was produced from a set of nine horizontal cuts (right ascension versus velocity) and 13 vertical cuts (declination versus velocity) through the full-resolution maps. At each of the intersections of this grid, the velocity of the dominant feature was determined by hand. Isovelocity

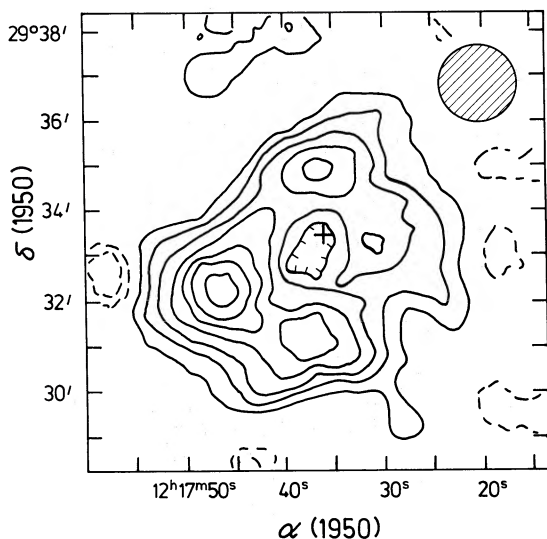


FIG. 2a

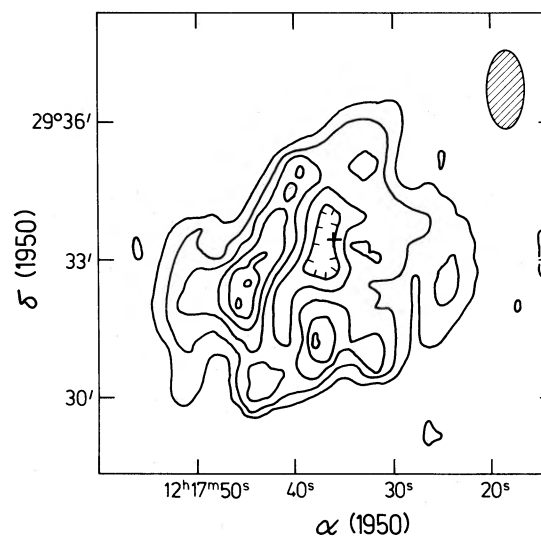


FIG. 2b

FIG. 2.—(a) The distribution of the total column density of neutral hydrogen in NGC 4278 obtained by integrating the smoothed maps. The beam size is indicated in the upper right-hand corner. The contour interval is  $2.37 \times 10^{19} \text{ cm}^{-2}$ . Negative contours are dashed; the zero contour is not given. The cross indicates the position of the nuclear source. (b) Neutral hydrogen distribution in NGC 4278 obtained by integrating the full-resolution maps over those areas where  $T_b > 0.15 \text{ K}$  in the smoothed maps. The contour interval is  $3.79 \times 10^{19} \text{ cm}^{-2}$ .

contours were drawn in later. Although, in general, the former method of calculating a velocity field is the most unbiased one, it produces a result which is difficult to interpret when the angular resolution does not match the velocity resolution, as is the case in the current observations. In particular near the center of the galaxy and near the minor axis, one beam of  $103 \times 103$  arc seconds contains emission from hydrogen from the ap-

proaching as well as from the receding half of the galaxy, thus smoothing the velocity field undesirably. This can easily be verified by comparison with Figure 3. Despite this handicap the most prominent feature of the velocity field, the nonperpendicularity of the kinematical major and minor axes, is shown equally well by both velocity fields.

In Figure 5b (Plate 6) the velocity field of Figure 4b is superposed on an optical photograph for comparison. The parts of the isovelocity contours drawn as solid lines are considered to be relatively unaffected by beam smearing. A compilation of the relevant information on NGC 4278 and its neighbor NGC 4283 obtained from previous observations and from the present data (on NGC 4278 only) is given in Table 2. Distances and linear dimensions were calculated using a Hubble constant of  $50 \text{ km s}^{-1} \text{ Mpc}^{-1}$ .

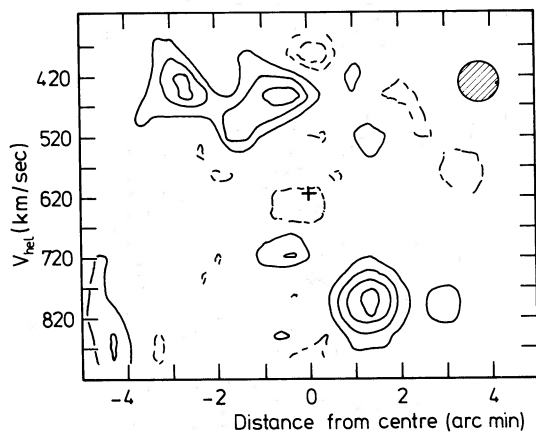


FIG. 3.—Distribution of H I velocities along a cut through the center of NGC 4278 at position angle  $65^\circ$  (SW to NE). This position angle corresponds to that of the apparent kinematical major axis of the hydrogen ring. The contour interval is  $0.2 \text{ K}$  of brightness temperature. The resolution in position and velocity is shown in the upper right-hand corner. At a distance of  $16.4 \text{ Mpc}$   $1'$  corresponds to  $4.8 \text{ kpc}$ .

#### b) Comparison with Earlier Observations

The neutral hydrogen in NGC 4278 has been observed before using five different telescopes: the Nancay  $200 \times 40 \text{ m}$  telescope (Bottinelli and Gouguenheim 1977a), the NRAO  $43 \text{ m}$  telescope (Gallagher *et al.* 1977), the NRAO  $91 \text{ m}$  telescope (Gallagher *et al.* 1977), the Arecibo  $300 \text{ m}$  telescope (Knapp, Kerr, and Williams, 1978), and the Effelsberg  $100 \text{ m}$  telescope (Bieging 1978). In principle, the current observations may be compared with the others on four points: (i) total flux (or H I mass), (ii) shape and width of the integrated profile, (iii) H I distribution, and (iv) kinematics. The latter two comparisons are possible only

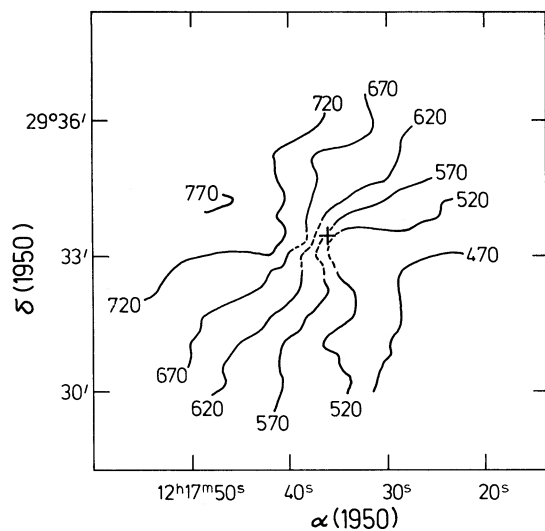


FIG. 4a

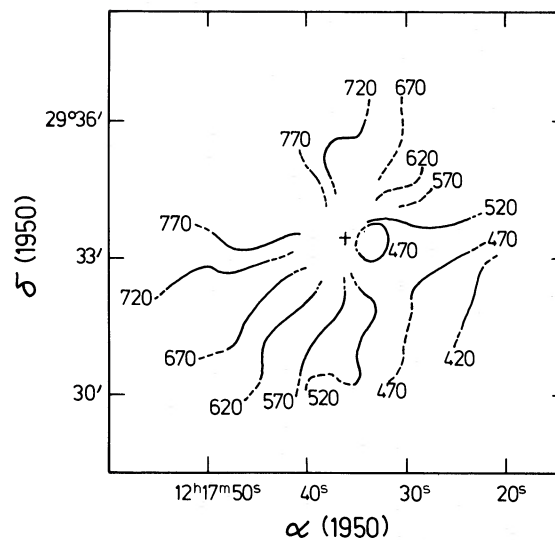


FIG. 4b

FIG. 4.—(a) Isovelocity contours of the H I gas around NGC 4278. The mean velocity at every point in the smoothed maps was determined by weighting each velocity with the local brightness temperature at that velocity and taking the weighted mean of these velocities. As a result of the poor angular resolution of the data, this process yields a velocity distribution badly affected by beam smearing. (b) The H I velocity field of NGC 4278 was obtained by determining the velocity of the dominant feature at approximately 100 points in the map by inspecting 9  $\alpha - V$  cuts and 13  $\delta - V$  cuts through the full-resolution data. The contours are shown as full lines over the area inside the 0.3 K ( $\sim 6 \sigma$ ) contour at the corresponding frequency (cf. Fig. 1) and as dashed lines between the 0.2 and 0.3 K contours.

TABLE 2  
OBSERVATIONAL INFORMATION ON NGC 4278 AND NGC 4282

| Parameter  | NGC 4278                       | NGC 4283                |
|--|--------------------------------|-------------------------|
| Optical redshift <sup>a</sup>                            | 474 km s <sup>-1</sup>         | 1125 km s <sup>-1</sup> |
| H I redshift <sup>a</sup>                                | 508 km s <sup>-1</sup>         | ...                     |
| Group redshift <sup>a, b</sup>                           | 822 km s <sup>-1</sup>         | 822 km s <sup>-1</sup>  |
| Distance   | 16.4 Mpc                       | 16.4 Mpc                |
| $B_T$  | 11.15 mag                      | 12.95 mag               |
| Absolute $B$ magnitude                                   | -19.92 mag                     | -18.12 mag <sup>9</sup> |
| $L/L_\odot$  | $1.45 \times 10^{10}$          | $2.76 \times 10^9$      |
| H I mass   | $7.4 \times 10^8 M_\odot$      | ...                     |
| Total mass within 12.9 kpc                               | $> 1.3 \times 10^{11} M_\odot$ | ...                     |
| $M/L_B$ within 12.9 kpc                                  | $> 9$                          | ...                     |
| Position angle of H I kinematic major axis               | $65^\circ \pm 5^\circ$         | ...                     |
| Position angle of H I kinematic minor axis               | $140^\circ \pm 3^\circ$        | ...                     |
| Position angle of elongated H I ring                     | $135^\circ$                    | ...                     |
| Position angle of optical axis                           | $20^\circ$                     | ...                     |
| Parameters of Oval Orbit Model                           |                                |                         |
| Position angle of kinematic major axis                   | $65^\circ$                     | ...                     |
| Position angle of line of nodes ( $\phi$ )               | $66^\circ$                     | ...                     |
| Angle between ascending node and major axis ( $\theta$ ) | $35^\circ$                     | ...                     |
| Inclination ( $i$ )                                      | $45^\circ$                     | ...                     |
| Axial ratio ( $b$ )                                      | 0.67                           | ...                     |
| Position angle of projected minor axis                   | $21^\circ$                     | ...                     |

<sup>a</sup>Corrected for motion of galaxy in Local Group.

<sup>b</sup>Based on membership of group No. 53 in Turner and Gott 1976.

between the Arecibo and the current Westerbork observations as an integrated line profile was measured in the other three cases.

i) *Total Flux*

Table 3 lists the total fluxes, the line widths and the H I masses based on a distance of 16.4 Mpc for NGC 4278 for the five sets of observations. The agreement of the current observations with the NRAO 91 m and the Arecibo results is very good. Considering the uncertainty in the baseline of the spectrum and the spurious instrumental problem noted by the observers of the NRAO 43 m telescope, that result also agrees with ours satisfactorily. The Nancay and the Effelsberg total fluxes are considerably lower than the others. This is possibly partly due to baselines curvature. Resolution of the H I complex by the large single dishes ( $>90$  m) could also account for some loss of total flux since the hydrogen tends to be distributed toward the outside of a ring whose size is comparable to or larger than the beam sizes of these dishes. This does not apply to the Arecibo observations as they were taken at a raster of points around the center of the galaxy.

ii) *Profile Shape*

Comparison of the integrated line profile constructed from the WSRT observations by summing the profiles over the relevant area of sky (Fig. 6) with the published profiles of the other telescopes suggests the following remarks:

a) The agreement of the observations with comparable combinations of collecting area, noise temperature, and integration time (WSRT, Nancay, NRAO 43 m, Effelsberg, and Arecibo) is fair. Even the much noisier NRAO 93 m profile agrees with the others in a qualitative manner, and in retrospect it is perhaps understandable that Gallagher *et al.* (1977) did not recognize the double-peaked structure in their data. However, their speculations which were based on an assumed Gaussian shape for the profile are obviously no longer relevant.

b) The relative heights of the two peaks in the profile are different as seen by the different telescopes. This is probably due to the fact that the main contributor to the high-velocity peak is the massive H I complex in the SE

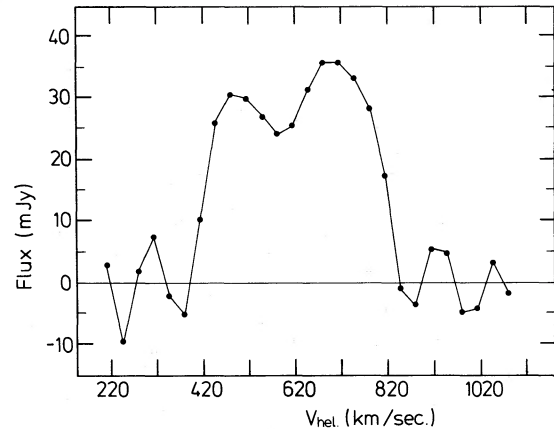


FIG. 6.—Line profile of the integrated 21 cm radiation of NGC 4278 obtained by summing the flux densities per velocity over the relevant area of sky. This profile may be compared with those obtained by other authors using single dishes.

quadrant of the galaxy (see Fig. 1). Obviously, the observed height of this peak is quite sensitive to the beam size and the pointing performance of the bigger single dishes.

iii) *H I Distribution*

In order to compare the H I distribution as observed with the WSRT and with the Arecibo telescope, we convolved the higher-resolution WSRT results to a  $3'$  circular beam. The result is shown in Figure 7. Three things are clear: (a) The central minimum in the H I distribution found in the current observations could not possibly have been seen with the resolution of the Arecibo telescope, as indeed it was not. (b) The peak of the convolved Westerbork map does not coincide with the peak of the Arecibo gas distribution. The difference is  $2:3$  mainly in the E-W direction. (c) The large E-W extent of the distribution as indicated by Knapp, Kerr, and Williams (1978) is not confirmed by the Westerbork observations.

We do not believe that the E-W elongation in the distribution seen in the Arecibo data is due to an asymmetrical antenna sidelobe pattern at Arecibo, as Knapp and coworkers checked the beam pattern and

TABLE 3  
NGC 4278 OBSERVED BY DIFFERENT TELESCOPES

| Telescope      | Size (m)        | $S(V) dV$ (Jy km s $^{-1}$ ) | $M_{\text{H I}}$ ( $M_{\odot}$ ) | $\Delta V$ (km s $^{-1}$ ) |
|----------------|-----------------|------------------------------|----------------------------------|----------------------------|
| NRAO .....     | 43              | 8.3                          | $5.0 \times 10^8$                | 520                        |
| NRAO .....     | 91              | 11.9                         | $7.2 \times 10^8$                | 470                        |
| Effelsberg ... | 100             | 4.1                          | $2.6 \times 10^8$                | 400                        |
| Nancay .....   | 200 $\times$ 40 | 4.3                          | $2.7 \times 10^8$                | 510                        |
| Arecibo .....  | 300             | 11.5                         | $7.3 \times 10^8$                | 470                        |
| WSRT .....     | ...             | 11.7                         | $7.4 \times 10^8$                | 400                        |

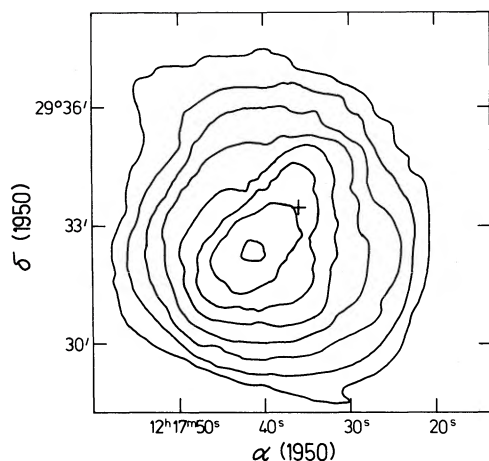


FIG. 7.— Total hydrogen distribution convolved with a circular beam of 3' diameter which yields a resolution comparable to that of the Arecibo 300-m dish. Contour intervals are  $1.18 \times 10^{19} \text{ cm}^{-2}$  in neutral hydrogen column densities. The cross indicates the position of the nuclear source.

found it to have approximately circular symmetry. However, other factors might play a role. Chief among these is the fact that, at Arecibo, the column density detection limit is lower in regions where the line profile is narrow, especially when nonlinear fits are made to the baselines, the procedure used by Knapp, Kerr, and Williams (1978). This effect could overweight regions along the kinematic major axis and thus swing the long axis of the surface density distribution into the E-W direction.

For the considerably larger angular extent of the gas seen at Arecibo, however, we have no airtight explanation. In principle, very extended structures could be missed by the WSRT as it has less collecting area and is therefore less sensitive to low-surface-brightness structures, and, at its shortest baseline of 36 m, features exceeding about 6' on an individual channel map begin to be attenuated. However, the excellent agreement between the total fluxes observed by both telescopes seems to preclude the existence of a large amount of gas unseen by Westerbork. Perhaps the seemingly larger extent of the Arecibo gas distribution is due to the very significant sidelobes of the Arecibo pattern, or alternatively to modest pointing errors. Repeat observations of NGC 4278 at Arecibo have recently been made by D. Burstein and N. Krumm (private communication) using the new feed having lower sidelobes. The origin of the Arecibo-Westerbork discrepancy may be better understood once these new data have been studied.

#### iv) Kinematics

The kinematic properties as described by Knapp, Kerr, and Williams (1978) are well confirmed by the current observations. The position angle of the kinematic major axis found from the two sets of observa-

tions coincide within the errors, while the position angle of the kinematic minor axis could hardly be determined from the Arecibo observations. In the region where they can be compared, both rotation curves seem to agree satisfactorily.

### III. DISTRIBUTION AND KINEMATICS OF THE NEUTRAL HYDROGEN

#### a) General Characteristics

What clues do these new observations provide to the origin of gas in NGC 4278? Before tackling this difficult question, let us begin with a descriptive summary of the data. As stated above, the gas distribution is broadly regular, showing an elongated disk, probably with a central minimum. However, three important deviations from perfect symmetry are present. First, the center of the ring is displaced from the nucleus of the optical galaxy by roughly 30'' toward the southeast. This displacement appears in several independent velocity channels and thus appears to be real. Second, it seems likely that the distribution is irregular, although the details of the spatial irregularities are difficult to determine because of the limited signal-to-noise ratio of the data. Finally, there is considerably more gas in the SE quadrant as compared to the NW. This difference is also highly significant appearing as it does in several independent velocity channels. In short, although the gas is distributed roughly in an elongated disk, it cannot be accurately described by any model having simple spatial symmetry.

By contrast, the velocity field seems rather regular, displaying central symmetry about the center of rotation. The overall velocity pattern is consistent with a rotating gaseous disk or ring viewed at moderate inclination. However, one surprising feature is apparent: the dynamical major and minor axes are not mutually perpendicular. We have determined the position angles of the dynamical axes from the individual channel maps, with the results shown in Table 2. The angle between the axes is only  $75^\circ$ , significantly smaller than  $90^\circ$ . The lack of perpendicularity of the axes is obvious to the eye in both Figures 4a and 4b.

This skewing of the axes probably is not solely the result of beam smearing acting on an inhomogeneous H I distribution. Although this effect could conceivably account for some of the skewing (note that the skewing is more apparent in Fig. 4a, which has a lower resolution, than in Fig. 4b), it does not seem likely that it produces as large a misalignment as is observed. The skewing also appears in several independent velocity channels. It therefore seems to be a real feature of the galaxy and not just an observational effect. We believe that the skewing could be an important clue to the shape of the mass distribution around NGC 4278, as is discussed further in § IV.

### b) *Mass and Mass-to-Light Ratio*

As indicated in Figure 3, the rotation curve is basically symmetric about the center with a steep rise near the nucleus which is not resolved by our beam. In the SW quadrant, gas is detected over a significant range of radii, and the rotation curve seems to be rather flat, as in later-type spirals. The observed rotational velocity can be used to set very rough limits on the mass-to-light ratio of NGC 4278. Gas is detected out to a maximum radius of 2.7, or 12.9 kpc, along the major axis in the SW quadrant (see Table 2). Estimating the inclination of the gaseous disk to the plane of the sky is difficult owing to the general lack of symmetry in the H I distribution. However, since the clear existence of the central hole indicates that the gas cannot be seen extremely edge-on, a plausible upper limit to  $i$  would seem to be roughly  $60^\circ$ . We therefore find a total mass of more than  $1.3 \times 10^{11} M_\odot$  within 12.9 kpc.  $M/L_B$  computed on the system of Faber and Gallagher (1979) is then  $>9$  within the same radius (see Table 2).

Nuclear values of  $M/L_B$  in elliptical galaxies as summarized by Faber and Gallagher (1979) average around 8.5, but Schweizer's (1979) recent estimates of seeing corrections to elliptical core profiles indicate that this average should be reduced by about 25%. Hence, if NGC 4278 is typical, its nuclear  $M/L_B$  would be about 6.4, somewhat smaller than the lower limit of 9 found at 12.9 kpc. The present observations thus hint at a rise in mass-to-light ratio in the outer regions, which would be consistent with the flat rotation curve. Unfortunately, the uncertainty is large as the magnitude of the effect depends crucially on the adopted inclination; it is unfortunate that this important quantity cannot be better determined from the present data.

### c) *Orientation of the H I with Respect to the Underlying Optical Galaxy*

Optical observations of NGC 4278 have established that the dynamical major axis of both gas and stars within  $40''$  of the nucleus is roughly coincident with the optical major axis of the galaxy, which has a position angle of approximately  $20^\circ$ . This important fact was originally shown by Osterbrock (1960) for the inner ionized gas. At our request, Joseph Miller has generously measured his more recent photographic prime-focus spectra of NGC 4278 taken with the Lick Observatory 3 m telescope, on which  $\lambda 3727$  of [O II] is prominent. These spectra indicate a rotational velocity of  $140 \text{ km s}^{-1}$  at a distance of  $6''$  along the major axis, with the NE quadrant receding. At a distance of  $36''$  from the nucleus the velocity has risen to  $245 \text{ km s}^{-1}$ , although the uncertainty here is large because the emission line is weak. Along the minor axis no rotational motion could be detected.

From higher-quality H $\alpha$  observations made with the Image Photon Counting System of University College London a provisional value of  $37^\circ$  for the position angle of the kinematical major axis of the ionized hydrogen has been derived by Boksenberg, Butcher, and Ulrich (in preparation).

The rotation of the stellar component in NGC 4278 has been studied by Schechter and Gunn (1979), who measured rotation curves in position angles  $0^\circ$ ,  $22^\circ$ , and  $90^\circ$ . They found moderate rotation speeds of  $40\text{--}50 \text{ km s}^{-1}$  in position angles  $0^\circ$  and  $22^\circ$ . These values are similar to those found along the major axis of other normal elliptical galaxies (Illingworth 1977; Davies 1979). Like the gas, the stars are receding in the NE quadrant. In position angle  $90^\circ$ , which is close to the minor axis, near zero rotation is seen. In summary, although the kinematic major axis of the stars is not determined with high accuracy, it appears to be at least roughly aligned with the optical major axis.

The outer hydrogen gas appears to have a direction of rotation different from the stars and the gas in the inner regions of the galaxy. The present observations indicate a position angle of  $65^\circ$  for the kinematic major axis of the outer gas (Table 2),  $45^\circ$  away from the optical major axis (however, the sense of rotation is the same in the inner and outer portions of the galaxy, the NE quadrant receding in both cases).

An additional complication is introduced by the H I surface density distribution, which bears no obvious relation to either of these kinematic axes. This is perhaps not an unexpected result, as the H I distribution in the few gas-poor disk galaxies that have been mapped with high spatial resolution also appear to be patchy and irregular (Bosma, van de Hulst, and Sullivan 1977; Krumm and Burstein 1979), and large-scale irregularities are common even in gas-rich spirals (e.g., Bosma 1978). But in any case, there is certainly no indication of a symmetric ring with the major axis in position angle  $65^\circ$ , as one would have expected from the kinematic data alone.

## IV. KINEMATIC MODELS FOR THE H I

### a) *Oval-Orbit Model*

The preceding discussion of position angles in § IIIc, suggests that it may not be possible to find a simple model which simultaneously accounts for both the surface density distribution and the dynamics of the outer gas. In what follows, we have chosen to match the dynamical data rather than the density distribution for two reasons. First, the velocity field shows greater regularity, encouraging us in the belief that it is somehow physically more meaningful. Second, as we noted above, irregularities in the H I distribution may be a common, albeit unexplained, feature of galaxies. In such

cases the isodensity contours of the H I may not indicate mean orbital trajectories, as they do in the inner regions of spirals.

Relying then exclusively on the kinematic data, we hypothesize a flattened disk of gas whose basic motion is one of ordered, axial rotation. The other important kinematic feature to be accounted for is the skewing of the dynamical major and minor axes. Clearly, some velocity perturbation must be added to basic circular orbits in order to produce this effect. Skewing such as this is commonly seen in ordinary disk galaxies, most often barred spirals (e.g., Peterson *et al.* 1978; Bosma 1978). Bosma has successfully modeled the gas flow in such galaxies by assuming that the gas particles flow around the bar along oval orbits. Theoretical studies (e.g., Sanders and Huntly 1976; Roberts, Huntly, and van Albada 1979) confirm that gas orbits near bars are distorted into ovals. Furthermore, the gas flow pattern is found to be invariant with time in a coordinate system rotating with the pattern speed of the bar disturbance.

We have adopted this point of view in setting up a model for the gas motion around NGC 4278. We envision that each (noninteracting) particle follows an elliptical trajectory which is closed in some uniformly rotating coordinate frame. The free parameters in such a model are  $b$ , the axial ratio of the ellipse,  $v$ , the mean velocity of the particle around the ellipse in the corotating frame, and  $\Omega_p$ , the angular pattern speed of the corotating frame. The orientation of the ellipse is specified by its inclination  $i$  to the plane of the sky, the position angle  $\phi$  of the line of nodes, and the angle  $\theta$  between the ascending node and the major axis (see Fig. 8).

We also require an expression for the speed change of each particle around the ellipse. Particles would be expected to move most rapidly near the minor axis of the ellipse, where they are closest to the center of the galaxy. For real gas flows, it is difficult to model this speed change very accurately as there are likely to be complicating effects due to shocks. Flow trajectories are also likely to depart from true ellipses for the same reason. Our simple model based on noninteracting particles therefore lacks full realism and can at best serve as an intuitive aid in understanding the true situation.

Given the crudity of the present approach, it seems an adequate first step to approximate the speed variation using the epicyclic approximation. The assumption that the orbit is an exact ellipse yields the following approximate expression for the maximum fractional velocity variation around the orbit:

$$\left| \frac{\Delta v}{v} \right|_{\max} \approx \frac{3}{2} \frac{1-b}{1+b} \quad (1)$$

Here  $\Delta v$  is positive at perigalacticon and negative at apogalacticon. For resonant particles in a flat rotation

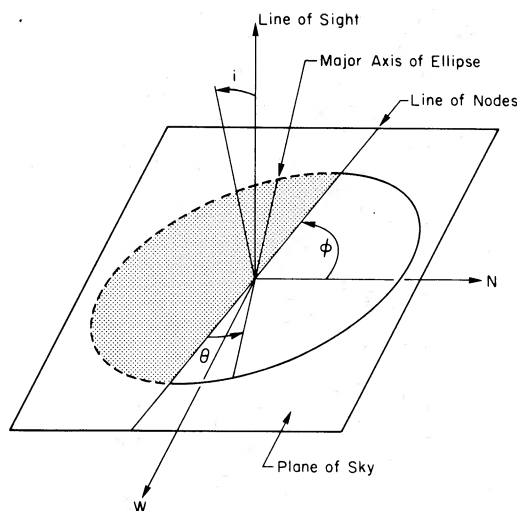


FIG. 8.—Figure illustrating the geometry of a model elliptical ring of gas surrounding NGC 4278. The ellipse is tilted with respect to the plane of the sky by an angle  $i$ . Angle  $\theta$  is measured in the plane of the ellipse, angle  $\phi$  in the plane of the sky.

curve, the pattern speed is given by (Mihalas 1968):

$$\Omega_p = \left( 1 - \frac{1}{\sqrt{2}} \right) \Omega, \quad (2)$$

where  $\Omega$  is the observed mean angular rotation rate of the outer gas.

Although the accuracy of the present data is not adequate to fully constrain such a model, useful limits can be placed on certain of the parameters. The velocity field and the H I surface density distribution for a sample model are shown in Figures 9a and 9b and the model parameters appear in Table 2. The axial ratio of 0.67 for the ellipse in this model is about as close to unity as is allowed. The inclination of  $45^\circ$  is well within the plausible limits discussed above. The longitude of  $35^\circ$  for the ascending node cannot be changed by more than  $\pm 15^\circ$  without altering the skewing angle by an unacceptably large amount. Finally, as is true of all models for the velocity field, the true major axis of the ellipse lies within the acute angle between the apparent kinematical axes, while the true minor axis lies within the obtuse angle.

Although the model fits the velocity field fairly well, it is of little help, as we already suspected, in understanding the surface density distribution of the gas, which is elongated in a quite different direction (compare Figs. 2 and 9b). However, the situation may be similar to, but slightly more extreme than, that in NGC 4736 (Bosma, van de Hulst, and Sullivan 1977), an outer-ring Sab galaxy. In this object, the outer ring is unevenly filled with gas, with a buildup at opposite ends of the minor axis of the ring. If observed with a relative

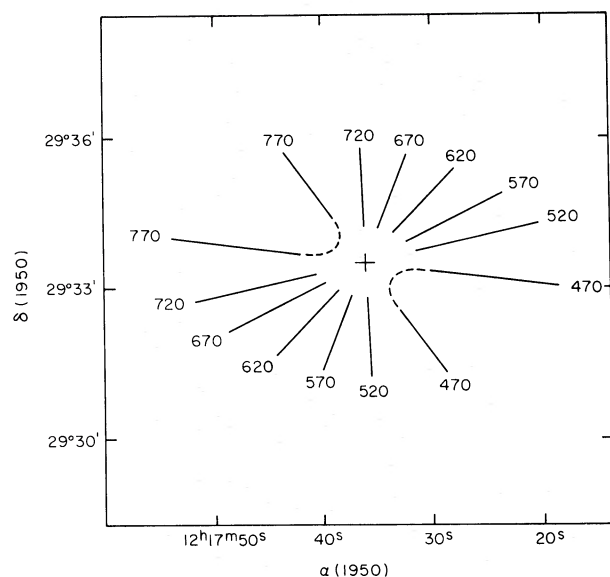


FIG. 9a

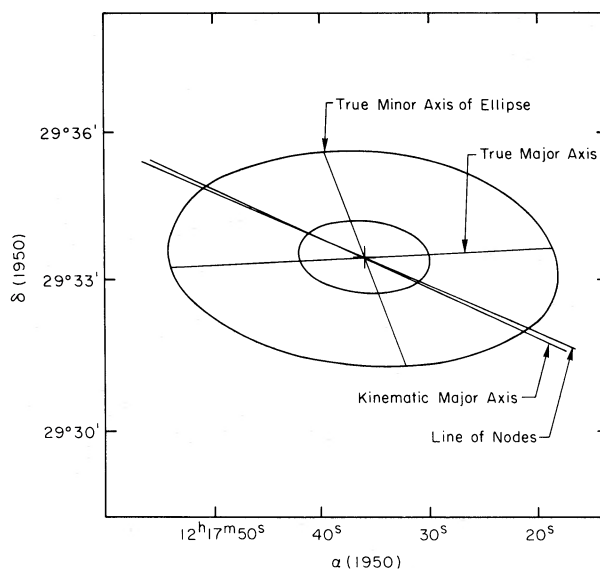


FIG. 9b

FIG. 9.—(a) Model velocity field of elliptical ring described in the text and illustrated in Fig. 8. A flat rotation curve having a maximum projected rotational velocity of  $\pm 180 \text{ km s}^{-1}$  was assumed. (b)—Appearance of model elliptical ring projected on the plane of the sky. Shape and orientation of the ring are to be compared with the observed gas distribution in Fig. 2.

angular resolution as low as that used for NGC 4278, the H I distribution in this ring would appear to be elongated perpendicular to the optical major axis of the ring, rather like the situation required by the oval-orbit model for NGC 4278.

To conclude, although the lack of fit to the surface-density distribution in NGC 4278 is certainly not evidence in favor of the oval-orbit model, it is perhaps not overwhelming evidence against it either. H I observations at higher sensitivity and angular resolution would greatly help to clarify the true H I distribution and perhaps to pick out tenuous clumps of gas populating the rest of the ring, if it really does exist.

#### b) Other Models

We have considered several other models, none of them outstandingly successful, for the origin of the skewing of the dynamical axes in NGC 4278. The first is based on the fact that the orbit of the outer gas should precess if the central galaxy is oblate and if the orbital plane of the gas is inclined with respect to the equatorial plane of the oblate plane. Calculations indicate that precession of a circular orbit will produce a tilting of the dynamic axes but that the angle between them will remain  $90^\circ$ . This result may be understood intuitively once it is noticed that a skewing of the axes requires a velocity perturbation having a  $\cos 2\xi$  dependence, where  $\xi$  is the angle around the orbital plane. It is easy to show that a velocity perturbation due to a single precessing ring has a  $\cos \xi$  dependence and so produces a tilt of the axes but no skewing. Expansion or contrac-

tion of a ring of gas is unable to cause skewing for exactly the same reason.

The model proposed by Sanders (1980), in which gas originating from stellar mass loss collapses toward the center of the E galaxy, predicts a velocity field with skewed axes. However, it is hard to see why we would find this collapsing gas in the outer regions of the galaxy where the density of stars is low.

Warp models offer an alternative possibility at the cost of added complexity. As discussed by Bosma (1978) in his extensive compendium of 21 cm velocity fields, motions in warps and in bar-shaped potentials can look strikingly similar. The success of the bar model in matching the velocity field of NGC 4278 suggests that its close relative—the warp—also be considered seriously.

After careful comparison of several barred and warped galaxies, Bosma was able to offer two purely dynamical criteria for distinguishing between the two types of motion. With a warp, the kinematic major and minor axes remain perpendicular, especially at the center of the galaxy, whereas with a bar, the axes are skewed at the center. With a warp, the kinematic minor axis also exhibits a characteristic S-shaped deformation with a matching S-shaped wave along the major axis at corresponding radii. For a bar, observed with the rather low spatial resolution which often typifies 21 cm studies, the minor axis deviation tends to disappear while the major axis kink remains (cf. Sancisi, Allen, and Sullivan 1979).

According to both of these criteria, the velocity field in NGC 4278 seems to resemble oval motion in a

bar-shaped potential more strongly than it does a warp. This conclusion could be voided, however, if the velocity field of a warped galaxy was incompletely filled with gas. For example, if the center was empty and if gas along the minor axis was physically located at much greater distances from the nucleus than the gas along the major axis, spurious skewing could appear when none really existed. (Much the same reasoning could be invoked to save the precession and expansion-contraction models as well.)

Although this possibility cannot be conclusively ruled out, it seems unlikely because there is gas present at a large range of radii along the SW kinematic major axis. Unless the inclination exceeds the plausible upper limit of  $60^\circ$ , it seems that this gas along the major axis does not in fact lie significantly closer to the nucleus than the gas along the minor axis. The requirements of the model therefore do not appear compatible with the observed gas distribution. Further observations at higher sensitivity to detect gas at larger and smaller radii along the major axis would be helpful in testing this tentative conclusion.

A further possible influence upon the gas disk in NGC 4278 is tidal interaction with NGC 4283. This companion galaxy can be seen in Figures 5*a* and 5*b*, and its properties appear in Table 2. The present projected separation between the galaxies is 16.2 kpc, and the projected angular momentum of NGC 4283 about NGC 4278 is similar to that of the gaseous disk. Further, the position angle of NGC 4283 with respect to NGC 4278 is  $68^\circ$ , only  $3^\circ$  different from that of the kinematic major axis of the disk. Thus it seems possible that the misalignment between the gas disk and the underlying optical galaxy is due to the tidal influence of NGC 4283.

On the other hand, the skewing of the kinematic axes of the disk still remains a mystery at least within the framework of the impulsive approximation (Spitzer 1958) for the tidal encounter, which would predict only a  $\cos \xi$  component and not the  $\cos 2\xi$  component necessary for skewing. In any real tidal encounter, these asymmetries could conceivably develop with time, yet no arcs or plumes of luminous material commonly seen near tidally interacting galaxies are visible in this case. All in all, the evidence for or against a tidal disturbance appears inconclusive at present.

#### V. IMPLICATIONS OF THE OVAL-ORBIT MODEL

Since at present the oval-orbit seems able to account most naturally for the kinematic properties of NGC 4278, it is worthwhile exploring its implications a bit further. We have seen that oval orbits require a perturbation to the gravitational potential like that seen in barred spirals. As mentioned above, real barred spirals show a skewing of their kinematic axes similar to that seen in NGC 4278. Furthermore, the barred spirals of

earliest type (SB0–SBa) are often accompanied by an outer ring similar in shape to the oval orbit required in NGC 4278. Kormendy (1979) has found that the mean axial ratio of such rings is 0.74, close to the value of 0.67 in our sample model for NGC 4278. The outer rings in barred early-type galaxies are also often hydrogen rich (Bosma 1978; Mebold *et al.* 1979). Bosma has speculated that the outer ring represents a local minimum in the gravitational potential of the bar, like that found in the theoretical calculations of MacMillan (1958) and de Vaucouleurs and Freeman (1972). The gas could be trapped in this local potential minimum.

As this brief summary shows, there are several strong parallels between the dynamical properties of the H I in NGC 4278 and in barred outer-ring galaxies. Is it possible that NGC 4278 is simply an earlier-type analog of outer-ring S0 and Sa galaxies? In developing this picture the first task is to identify the bar, which in ordinary outer-ring galaxies is usually prominently visible in optical photographs. However, NGC 4278 shows no sign of a bar, or any other unusual discontinuities in its light distribution for that matter. From photometric analysis of the photographs shown here, plus others, Gunn (1981) reports that the luminosity profile of NGC 4278 follows a normal de Vaucouleurs law as far out as the surface brightness can be reliably measured.

Even though no clear bar is visible, the galaxy itself is somewhat elongated. If it were prolate instead of oblate, it could perhaps generate the requisite barred potential field. Interestingly enough, the optical major axis of NGC 4278 is in the proper orientation for this to occur. Kormendy (1979) and Gallagher (1981) find that in barred-outer-ring galaxies, the minor axis of the outer ring is oriented approximately parallel to the bar. In our dynamical models, we found that the minor axis of the oval ring was rather ill-determined, being allowed to vary by  $\pm 20^\circ$ . Curiously, however, the middle of the allowed range is virtually parallel to the optical major axis of NGC 4278. This alignment is nicely illustrated by our sample model in Figure 8. Under this interpretation, then, the visible galaxy would be a prolate spheroid analogous to the bars in SB0 and SBa galaxies, an intriguing result in view of the current controversy surrounding the true shapes of elliptical galaxies (e.g., Binney 1978; Marchant and Olson 1979).

Incidentally, the presence of a barred gravitational potential could be an important clue to the link between the nuclear activity in NGC 4278 and the outer H I. That these phenomena may be related has been discussed by a number of authors (Gallagher *et al.* 1977; Knapp, Gallagher, and Faber 1978; Fosbury *et al.* 1978; Gunn 1979). It is generally thought that the nuclear gas is derived somehow via gaseous inflow from the outer reservoir, but the main problem is how to remove angular momentum so that the gas can flow inward. Gunn (1979) has suggested a model in which the necessary

gaseous inflow is driven by viscous transfer of angular momentum between differentially precessing gaseous rings at different radii. This model successfully predicts a central hole in the gas distribution in NGC 4278 of about the right diameter.

The presence of a bar component in the potential could offer an alternative way to explain the inward flow. With a bar, gravitational forces on the gas will no longer be axisymmetric. A torque can be exerted on the gas, causing a net gain or loss of angular momentum. Recent calculations of gaseous flows near a bar (Roberts, Huntley, and van Albada 1979) show a net inward flow inside corotation with velocities of a few  $\text{km s}^{-1}$ . Perhaps such a mechanism fuels the nucleus of NGC 4278.

As the preceding discussion makes clear, the bar model for NGC 4278 has many attractive features. Unfortunately, however, there is also a severe problem: the available dynamical data indicate that the rotation of the inner optical galaxy is not coplanar with the outer gaseous ring. If objects in the inner galaxy were traveling in coplanar circular orbits, their kinematic major axis should be parallel to the line of nodes of the outer oval, which in all models is close to the kinematic major axis of the outer gas (see Fig. 8). To first order, the kinematic major axes in the inner and outer parts should therefore be coincident, not  $45^\circ$  apart as is observed (see § IIIc). To be sure, if the stars and gas in the inner galaxy were traveling on oval orbits of their own, as would be likely for particles within a bar, the projected kinematical major axis could be displaced slightly from the line of nodes. The effect would operate in the right direction (clockwise), but it seems unlikely that it could amount to the full shift of  $45^\circ$  needed here.

The only loophole left is the fact that the kinematic major axis of the stars is not very well known, there being only the spectra taken in three position angles by Schechter and Gunn (1979). An accurate determination of the stellar velocity field would thus be important in testing whether the optical galaxy really could be a rotating bar.

Pending such a study, however, the data as they now stand imply that the rotation of the central galaxy and the outer gas are not coplanar. Thus, if the central galaxy is a bar, it is tumbling with a component perpendicular to the plane of the outer gas, and the present alignment between the minor axis of the outer oval and the bar could be just a temporary coincidence. Furthermore, one would suspect that within a short time the orbit of the outer gas would be badly chewed up by the tumbling bar and the pleasing dynamical symmetry of the gaseous component thus rapidly destroyed. This problem might be avoided if the H I lies near the minor axis principle plane of a triaxial stellar system.

To carry these speculations one step further, it seems that these negative aspects of the bar model could also

be avoided if the barred component of the gravitational potential arises not in the optical galaxy but in a massive nonluminous envelope instead. This envelope would have to be prolate and coplanar with the outer gaseous ring. This possibility is most intriguing, yielding as it might an important clue to the shapes of massive nonluminous envelopes. Indeed, according to Binney (1978), the existence of warps in spirals is already strong evidence for triaxial invisible halos, and the presence of oval orbits in the exterior of NGC 4278 is precisely what might be expected on this line of reasoning.

In any case, it appears that the original simple analogy with SB0 and SBa galaxies has broken down, as the difference in direction of rotation between the inner and outer parts of the galaxy just seems too difficult to reconcile on this hypothesis. Any lingering doubts about this conclusion could be erased by accurate measurements of the stellar velocity field.

#### VI. REVIEW OF THEORIES FOR THE ORIGIN OF THE GAS

The present synthesis map of NGC 4278 was obtained primarily in order to test theories for the origin of the gas. On the basis of the rotational difference between the inner galaxy and the outer H I, Gallagher *et al.* (1977) and Knapp, Gallagher, and Faber (1978) argued that the gas was derived from the recent infall of an intergalactic H I cloud having an angular momentum vector different from the underlying galaxy. Although the situation seems to be considerably more subtle than was appreciated by these authors, owing to the fact that the possible presence of noncircular motions greatly complicates the interpretation of the dynamical axes, nevertheless the angular momentum vectors of the inner and outer galaxy do appear to be nonparallel. This is the central fact which must be accounted for by any successful model.

Since the idea of infall was first suggested by Gallagher *et al.* (1977), new observations have shown that the frequency of elliptical galaxies with detectable H I is not as small as was then supposed (Gouguenheim 1979). Moreover, searches for intergalactic H I clouds have shown them to be extremely rare (Lo and Sargent 1979; Shostak 1977; Haynes and Roberts 1979; J. A. Tully, unpublished). All in all, the frequency of accidental accretion of intergalactic H I now appears to be too small to explain the existence of gas in all the known ellipticals with H I (Bottinelli and Gouguenheim 1977b; Gouguenheim 1979).

On the other hand, although purely gaseous intergalactic clouds are rare, dwarf irregular galaxies have been discovered in surprising numbers with total gas content comparable to the H I mass in NGC 4278 (Fisher and Tully 1975). The optical luminosity of such objects is often exceedingly low (Thuan and Seitzer

1979*a, b*), and would be completely undetectable if spread out like the H I. It is therefore possible that in NGC 4278 we are witnessing the results from the capture of a dwarf irregular galaxy. This idea has been developed further in a recent paper by Silk and Norman (1979).

We must also point out that NGC 4278 is not unique in displaying two different axes of rotation. Shane (1980) has shown that the peculiar galaxy NGC 2685 also has two gaseous velocity systems, one aligned along the stellar velocity field and one nearly orthogonal to it. The bizarre properties of NGC 2685 strongly suggest a newly formed and short-lived configuration, and, indeed, Shane interprets this galaxy in terms of recent infall. Perhaps in NGC 4278 we are seeing a related but less extreme event.

If, on the other hand, we insist on a stable dynamical model for the gas, we can choose the incompletely filled warp model, perhaps an invisible, stabilizing, triaxial halo, or even admit the possibility of stable dynamical subsystems near the minor axis of triaxial systems. The first hypothesis can be tested by H I observations at higher sensitivity and resolution, which could reveal the characteristic S-shaped signature of a warp. The latter cases would best be tested by closely studying all other known gas-rich elliptical galaxies to see how common skewed dynamical axes are in such objects. If either stable model is valid, the gas would presumably be of ancient origin.

On the basis of the currently available information, we feel that the infall and triaxial halo models are the most likely candidates but that none of the other possibilities can be positively ruled out.

#### VII. SUMMARY AND CONCLUSIONS

Far from clarifying the situation, the present observations have raised more questions about the nature of the H I around NGC 4278 than they have answered. The important observational results are these: (*a*) the surface density distribution of the gas is roughly ring shaped but is irregular and cannot be fitted by any simple model; (*b*) the velocity field of the gas is fairly regular and, in large, indicates ordered rotation about the central galaxy; (*c*) slight evidence for a flat rotation curve is seen; (*d*) the kinematic major and minor axes of the gas are

skewed to one another; (*e*) the rotation of the outer gaseous ring does not appear to be coplanar with that of the optically visible inner galaxy.

Theoretically the most natural model for the skewing of the kinematic axes utilizes oval orbits for the motion of the outer gas. In this picture, the underlying gravitational potential would have a barred component, but due to point (*e*) above, the bar would have to originate in an invisible triaxial halo, not the optically visible E galaxy. Another attractive possibility involves recent accretion of external gas, possibly from a dwarf irregular galaxy. However, other hypotheses such as a warp or tidal perturbation by a companion cannot be rigorously ruled out.

Future observational studies should emphasize H I studies at higher resolution to search for the signature of a warp, to further delineate the clumpiness of the gas distribution, and to look for low-density clouds further out in the galaxy. An accurate map of the stellar velocity field is also needed to determine definitely whether the rotations of the inner and outer regions are in fact not coplanar. These observations and comparative studies of other H I-rich ellipticals should help to clarify the origin of these extraordinarily interesting and enigmatic galaxies.

We are especially grateful to Renzo Sancisi and Seth Shostak for their assistance in using the Groningen interactive system GIPSY, to Joseph Miller for his velocity measurements of the inner ionized gas, to James Gunn for the loan of his excellent photographic plates of NGC 4278 and to Alec Boksenberg, Harvey Butcher, and Marie Hélène Ulrich for making the provisional results of their observations available to us. Douglas Lin gave us invaluable help in working out the tidal and precession models. We thank Renzo Sancisi and Hugo van Woerden for their critical reading of the manuscript. This work was partially supported by the Alfred P. Sloan foundation, and by NSF grants AST 79-009977 and AST 77-18270 to the University of Illinois, and AST 79-16815 to the California Institute of Technology. The Westerbork Synthesis Radio Telescope is operated by the Netherlands Foundation for Radio Astronomy with the financial support from the Netherlands Organization for the Advancement of Pure Research (Z.W.O.).

#### REFERENCES

- Baars, J. W. M., and Hooghoudt, B. G. 1974, *Astr. Ap.*, **31**, 323.  
 Bieging, J. H. 1978, *Astr. Ap.*, **64**, 23.  
 Binney, J. 1978, *M.N.R.A.S.*, **183**, 779.  
 Bos, A., Raimond, E., and van Someren Grève, H. W. 1981, *Astr. Ap.*, in press.  
 Bosma, A. 1978, Ph.D. thesis, Groningen University.  
 Bosma, A., van de Hulst, J. M., and Sullivan, W. T. 1977, *Astr. Ap.*, **57**, 373.  
 Bottinelli, L., and Gouguenheim, L. 1977*a*, *Astr. Ap.*, **54**, 641.  
 ———. 1977*b*, *Astr. Ap.*, **60**, L23.  
 Casse, J. L., and Muller, C. A. 1974, *Astr. Ap.*, **31**, 333.  
 Davies, R. 1979, Ph.D. thesis, University of Cambridge.  
 de Vaucouleurs, G., and Freeman, K. C. 1972, *Vistas in Astronomy*, **14**, 163.  
 Faber, S. M., and Gallagher, J. S. 1979, *Ann. Rev. Astr. Ap.*, **17**, 135.  
 Fisher, J. R., and Tully, R. B. 1975, *Astr. Ap.*, **44**, 151.  
 Fosbury, R. A. E., Mebold, M., Goss, W. M., and Dopita, M. A. 1978, *M.N.R.A.S.*, **183**, 549.  
 Gallagher, J. S. 1981, in preparation.  
 Gallagher, J. S., Knapp, G. R., Faber, S. M., and Balick, B. 1977, *Ap. J.*, **215**, 463.

- Gouguenheim, L. 1979, in *Photometry, Kinematics and Dynamics of Galaxies*, ed. D. S. Evans (Austin: University of Texas), p. 102.
- Gunn, J. E. 1979, in *Active Galactic Nuclei*, ed. C. Hazard and S. Mitton (Cambridge: Cambridge University Press), p. 213.
- \_\_\_\_\_. 1981, in preparation.
- Haynes, M. P., and Roberts, M. S. 1979, *Ap. J.*, **227**, 767.
- Högbom, J. A., and Brouw, W. N. 1974, *Astr. Ap.*, **33**, 289.
- Illingworth, G. 1977, *Ap. J. (Letters)*, **218**, L43.
- Knapp, G. R., Gallagher, J. S., and Faber, S. M. 1978, *A. J.*, **83**, 139.
- Knapp, G. R., Kerr, F. J., and Williams, B. A. 1978, *Ap. J.*, **222**, 800.
- Kormendy, J. 1979, *Ap. J.*, **227**, 714.
- Krumm, N., and Burstein, D. 1979, *Bull. AAS*, **11**, 429.
- Lo, K. Y., and Sargent, W. L. W. 1979, *Ap. J.*, **227**, 756.
- MacMillan, W. D. 1958, *The Theory of the Potential* (New York: Dover).
- Marchant, A. B., and Olson, D. W. 1979, *Ap. J. (Letters)*, **230**, L157.
- Mebold, W., Goss, W. M., van Woerden, H., Hawarden, T. G., and Siegman, B. 1979, *Astr. Ap.*, **74**, 100.
- Mihalas, D. 1968, *Galactic Astronomy* (San Francisco: Freeman).
- Osterbrock, D. E. 1960, *Ap. J.*, **132**, 325.
- Peterson, C. J., Rubin, V. C., Ford, W. K., and Thonnard, N. 1978, *Ap. J.*, **219**, 31.
- Roberts, W. W., Huntley, J. M., and van Albada, G. D. 1979, *Ap. J.*, **223**, 67.
- Sancisi, R., Allen, R. J., and Sullivan, W. T. 1979, *Astr. Ap.*, **78**, 217.
- Sanders, R. H. 1980, *Ap. J.*, **242**, 931.
- Sanders, R. H., and Huntley, J. M. 1976, *Ap. J.*, **209**, 53.
- Schechter, P. L., and Gunn, J. E. 1979, *Ap. J.*, **229**, 472.
- Schweizer, F. 1979, *Ap. J.*, **233**, 23.
- Shane, W. W. 1980, *Astr. Ap.*, **82**, 314.
- Shostak, G. S. 1977, *Astr. Ap.*, **54**, 919.
- Silk, J., and Norman, C. 1979, *Ap. J.*, **234**, 86.
- Spitzer, L. 1958, *Ap. J.*, **127**, 17.
- Thuan, T. X., and Seitzer, P. O. 1979a, *Ap. J.*, **231**, 327.
- \_\_\_\_\_. 1979b, *Ap. J.*, **231**, 680.
- Turner, E. L., and Gott, J. R. 1976, *Ap. J. Suppl.*, **32**, 409.

S. M. FABER: Lick Observatory, University of California, Santa Cruz, CA 95064

J. S. GALLAGHER: Department of Astronomy, University of Illinois, Urbana, IL 61810

G. R. KNAPP: Department of Astrophysical Sciences, Princeton University, Princeton, NJ 08540

ERNST RAIMOND: Netherlands Foundation for Radio Astronomy, Postbus 2, 7990 AA Dwingeloo, The Netherlands

## PLATE 5

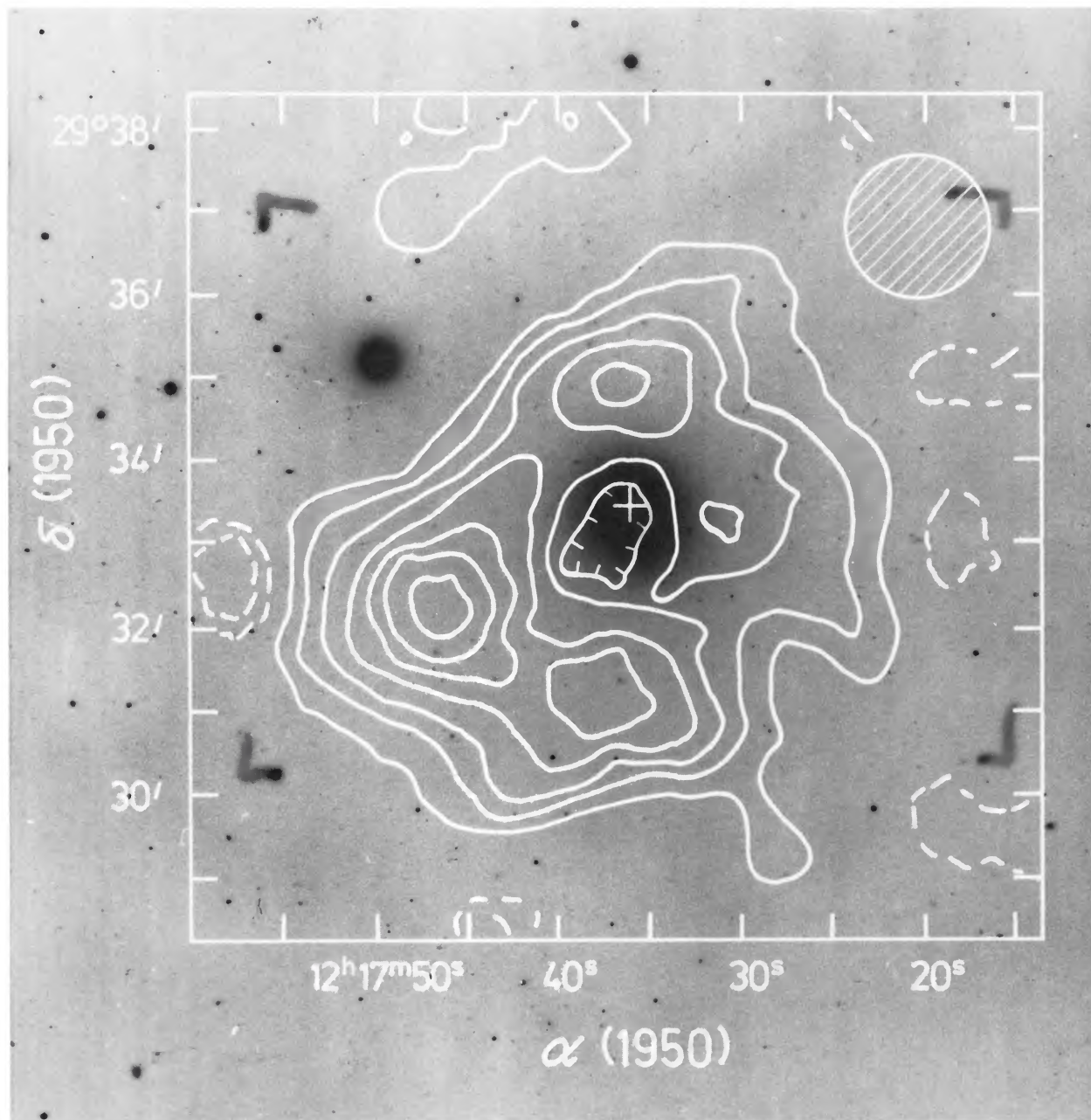


FIG. 5a.—H I distribution of NGC 4278 superposed on Palomar 5.08 m prime focus 098 photograph (kindly put at our disposal by James E. Gunn).

RAIMOND *et al.* (see page 709)

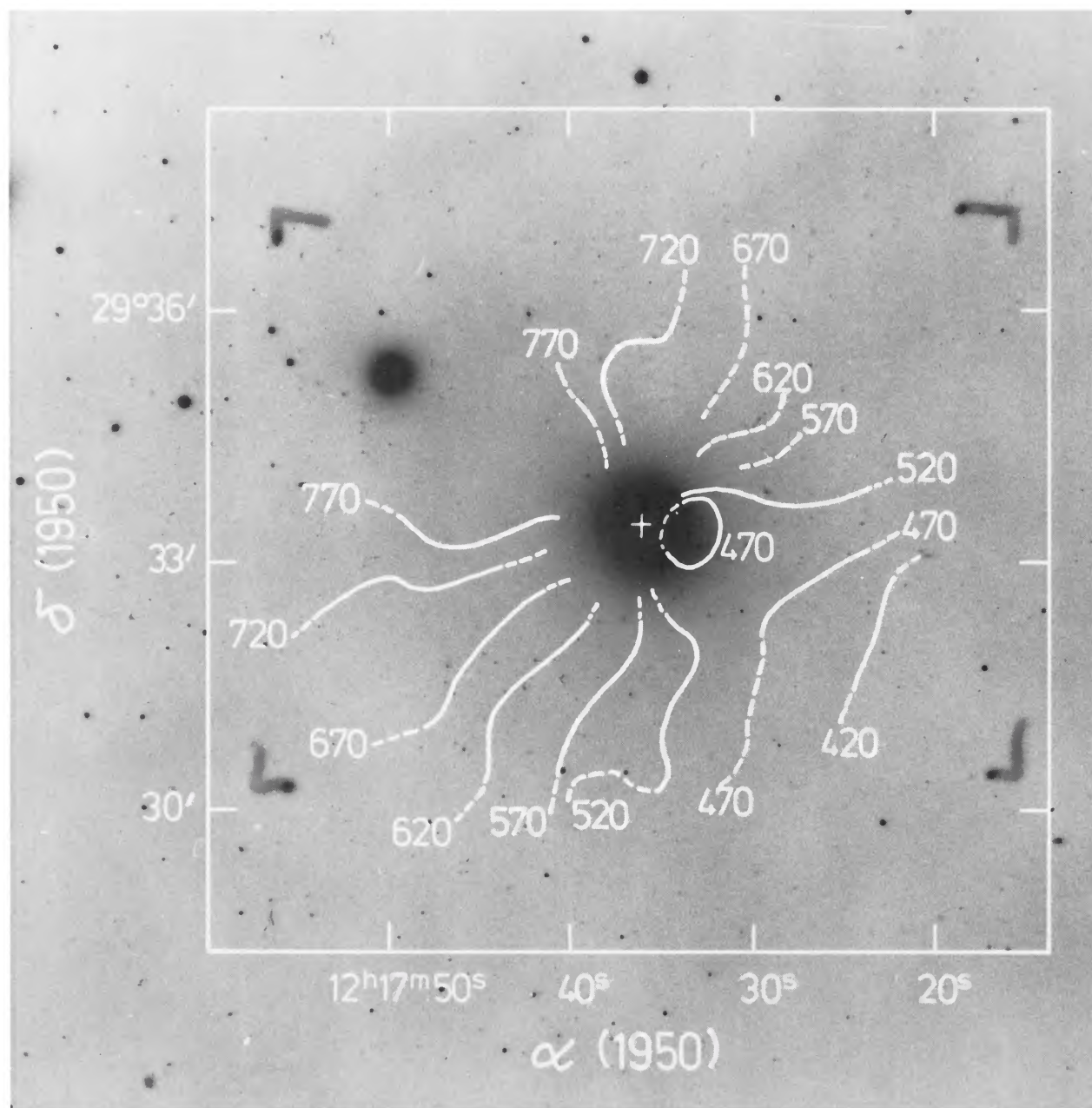


FIG. 5b.—Velocity field of NGC 4278 superposed on the same photograph

RAIMOND *et al.* (see page 711)